Incommensurate and collinear phases in a doped quantum antiferromagnet

1993 J. Phys.: Condens. Matter 5 8595

(http://iopscience.iop.org/0953-8984/5/45/012)

J. Phys.: Condens. Matter 5 (1993) 8595–8602. Printed in the UK

Incommensurate and collinear phases in a doped quantum antiferromagnet

W Barford and S Jadhav
Department of Physics, The University of Sheffield, Sheffield S3 7RH, UK

Received 21 June 1993, in final form 13 September 1993

Abstract. The Schwinger boson mean-field theories of the 't–J' model are extended by the consideration of anisotropic order parameters. This has two effects: first, a collinear phase in which the spins are antiferromagnetically aligned in one direction and ferromagnetically aligned in the other, is found to be stable over a significant range of the phase diagram; second, the (1, 1) and (1, 0) spiral phases become very close in energy. The inclusion of weak intrasublattice coupling may therefore stabilize the (1, 0) spiral with respect to the (1, 1) spiral, thus harmonizing theory and experiment.

1. Introduction

It is both experimentally and theoretically established that the undoped high-temperature superconductors are described by a two-dimensional (2D) spin $\frac{1}{2}$ Heisenberg antiferromagnet. Three-dimensional coupling stabilizes the long-range Néel order to temperatures of roughly 300 K. Upon doping, however, the long-range order is soon destroyed to be replaced by short-range antiferromagetic correlations, which are either incommensurate, as in $La_{2-x}Sr_xCuO_4$ [1], or commensurate, as in $YBa_2Cu_3O_{7-\delta}$, for example.

There have been many theoretical attempts to explain this behaviour. One approach is to treat the spins semi-classically. The hole motion then leads to a (1, 1) spiral distortion of the spin background [2, 3]. Another approach is a weak coupling RPA calculation in which the most divergent terms in the magnetic susceptibilty arise from the Fermi surface nesting wavevectors [4]. This approach has the virtue of explicitly building in the Fermi surface structure, and hence is easily able to explain the discrepancies between different compounds from their different Fermi surfaces. However, it implicitly assumes the underlying existence of a Fermi liquid, which is somewhat at variance with normal state transport properties.

A further approach is to take the strong coupling limit and to use a slave representation to explicitly prohibit double occupancy. Of the two (formally equivalent) representations we elect to use the slave fermion–Schwinger boson representation in which the fermion degree of freedom controls the occupancy. This method correctly predicts long-range antiferromagnetism at half filling, and the Nagaoka ferromagnet for infinitesimally small doping and infinite coupling, so it is a natural starting point when considering doping.

The Schwinger boson method has been used previously to study the mean-field theory of the 't–J' model [5] (which we define shortly). It was found that doping leads to an incommensurate spiral along the (1, 1) direction, which is in contrast to the experimental results of Cheong *et al* [1] who found incommensurate spirals along the (1, 0) direction. The inclusion of a next-nearest-neighbour hopping term, however, leads to the stabilization of the (1, 0) spiral for some parameter ranges [6]. The mean-field theory without fluctuations also predicts long-range order for most doping values, whereas short-range correlations are observed. Later work has shown that the long-range order is destroyed by the fluctuations [7]. This theory therefore seems a promising one for a complete explanation of the phase diagram.

In most of the mean-field analyses it is customary to assume that the order parameters are isotropic. However, if this restriction is relaxed new phases are found which are energetically favourable. In particular, we find that there is a phase transition from the $(1,1)$ spiral to a collinear phase, in which the spins are antiferromagneticaly aligned in one direction and ferromagnetically aligned in the other, before the onset of ferromagnetism. Furthermore, the energy of the $(1,0)$ spiral becomes very close to that of the $(1,1)$ spiral. The plan of this paper is as follows: first we introduce the 't–J' model to establish notation; then, in section 2, we describe the Schwinger boson mean-field method. Section 3 contains our results, and we conclude in section 4.

The 't–J' model may be obtained from the Hubbard Hamiltonian by formally projecting out double occupied states, but allowing virtual states of double occupancy. This leads to a Heisenberg exchange term with a coupling constant, $J = 4t^2/U$. It is more convenient, however, to treat this as a model Hamiltonian with t and J as independent variables. The 't–J' model then reads:

$$H = -t \sum_{\langle ij \rangle \sigma} \tilde{c}^\dagger_{i\sigma} \tilde{c}_{i\sigma} + \mathrm{HC} + J \sum_{\langle ij \rangle} \left(\boldsymbol{S}_i \cdot \boldsymbol{S}_j - \frac{1}{4} n_i n_j \right) \tag{1}$$

where HC stands for Hermitian conjugate, and where $\tilde{c}_{i\sigma}$ acts only in the empty and singly occupied subspace, and is defined as $(1 - n_{i\bar{\sigma}})c_{i\sigma}$. The sum, $\langle ij \rangle$, is over nearest neighbours.

With the introduction of the singlet operator,

$$\Delta_{ij} = \frac{1}{\sqrt{2}} \sum_{\sigma} \mathrm{sgn}(\sigma) c_{i\sigma} c_{j\bar{\sigma}}$$

equation (1) can be rewritten as

$$H = -t \sum_{\langle ij \rangle \sigma} \tilde{c}^\dagger_{i\sigma} \tilde{c}_{i\sigma} + \mathrm{HC} - J \sum_{\langle ij \rangle} \Delta^\dagger_{ij} \Delta_{ij}. \tag{2}$$

2. Mean-field analysis

To handle the constraint of no double occupancy we adopt the slave fermion representation whereby the physical electron operator is factorized into a spinless fermion f_i, and the SU(2) Schwinger boson $b_{i\sigma}$, i.e.

$$c^\dagger_{i\sigma} = f_i b^\dagger_{i\sigma}.$$

The fermions and bosons necessarily satisfy the constraint

$$\sum_{\sigma} b^\dagger_{i\sigma} b_{i\sigma} + f^\dagger_i f_i = 1$$

and so we may therefore identify the $f_i^\dagger$ as creating a hole and $b_{i\sigma}^\dagger$ as creating a spin on the ith site. Using this representation (2) then becomes

$$H = -t\sum_{\langle ij\rangle\sigma} f_i f_j^\dagger b_{i\sigma}^\dagger b_{j\sigma} + \text{HC} - J\sum_{\langle ij\rangle}\left(1 - f_i^\dagger f_i\right)\Delta_{ij}^{b\dagger}\Delta_{ij}^{b}\left(1 - f_j^\dagger f_j\right) \tag{3}$$

where $\Delta_{ij}^b = \frac{1}{\sqrt{2}}\sum_\sigma \operatorname{sgn}(\sigma) b_{i\sigma} b_{j\bar{\sigma}}$.

We use the saddle point approximation to solve (3), and introduce the following mean-field order parameters [8]

$$Q_{ij} = \sum_\sigma \langle b_{i\sigma}^\dagger b_{j\sigma}\rangle \tag{4a}$$

$$F_{ij} = \langle f_i^\dagger f_j\rangle \tag{4b}$$

and

$$D_{ij} = \langle \Delta_{ij}^b \rangle. \tag{4c}$$

Q_{ij} is a measure of the ferromagnetic alignment between neighbouring spins. This is illustrated by noting that for classical spins represented by the unit vectors $\hat{\Omega}$ it is given by [3]

$$Q_{ij} = (1-\delta)\sqrt{\tfrac{1}{2}\left(1 + \hat{\Omega}_i\cdot\hat{\Omega}_j\right)}\exp\left(\mathrm{i}\hat{\omega}(\hat{\Omega}_i, \hat{\Omega}_j; \hat{z})\right) \tag{5}$$

where $\hat{\omega}(\hat{\Omega}_i, \hat{\Omega}_j; \hat{z})$ is the solid angle spanned by the two spins and the global axis of quantization. δ is the hole concentration, so $(1-\delta)$ is a mean-field estimate of the average local spin concentration. F_{ij} is a measure of the bosonic band width, while D_{ij} is the singlet order parameter, and hence measures the antiferromagnetic alignment. All of the order parameters are assumed to be translationally invariant, with Q and F being even and D being odd under a space inversion.

In general, we are at liberty to choose the ratio of Q_x and Q_y and allow D_x, D_y, F_x and F_y to be determined self-consistently. Setting this ratio to unity results in the $(1,1)$ spiral, while setting it to zero results in the $(1,0)$ spiral. Alternatively, we can choose the ratio of D_x and D_y, while the other four order parameters are then self-consistently determined. In particular, setting this ratio to zero results in the collinear phase. The term $J(1-f_i^\dagger f_i)(1-f_j^\dagger f_j)$ is replaced by its mean-field value $J_\delta = J(1-\delta)^2$.

By decoupling (3) with these order parameters the spin and charge degrees are freedom are decoupled and the following Hamiltonians for the charge and spin degrees of freedom are obtained

$$\tilde{H}^f = \sum_k (\epsilon_k^f + \lambda_f) f_k^\dagger f_k + tN(F_x Q_x + F_y Q_y) \tag{6a}$$

and

$$\tilde{H}^b = \sum_k \left(b_{k\uparrow}^\dagger, b_{-k\downarrow}\right)\begin{pmatrix} \lambda_b + M_k & \gamma_k \\ \gamma_k^* & \lambda_b + M_{-k}\end{pmatrix}\begin{pmatrix} b_{k\uparrow} \\ b_{-k\downarrow}^\dagger\end{pmatrix}$$
$$- \lambda_b N + J_\delta N(D_x^2 + D_y^2) - J_\delta(Q_x^2 + Q_y^2)N/4. \tag{6b}$$

Notice that (6*a*) and (6*b*) have been defined in the grand canonical ensemble to ensure that the constraints $\langle f_i^\dagger f_i \rangle = \delta$ (= hole doping) and $\sum_\sigma \langle b_{i\sigma}^\dagger b_{i\sigma} \rangle = 1 - \delta$ are satisfied on the average. This is done via the introduction of the fermionic and bosonic chemical potentials, λ_f and λ_b, respectively. We define

$$M_k = 2\left[\left(F_x t + \frac{Q_x J_\delta}{4}\right)\cos k_x + \left(F_y t + \frac{Q_y J_\delta}{4}\right)\cos k_y\right] \tag{7}$$

and

$$\gamma_k = \sqrt{2}\mathrm{i} J_\delta (D_x \sin k_x + D_y \sin k_y). \tag{8}$$

The fermionic Hamiltonian is trivially diagonalized giving the spectrum:

$$\epsilon_k^f = -2t(Q_x \cos k_x + Q_y \cos k_y) \tag{9}$$

while the bosonic Hamiltonian is diagonalized via a Boguilobov transformation. This must be handled with care because of the possibility of a gapless spectrum and hence Bose–Einstein condensation at zero temperature. For the wavevectors at which Bose–Einstein condensation *does not occur* a non-unitary transformation is employed [9] which yields the eigenfunctions

$$\left(\alpha_k^\dagger, \beta_k\right) = \left(b_{k\uparrow}^\dagger, b_{-k\downarrow}\right)\begin{pmatrix} \sqrt{\frac{\xi+1}{2}}\mathrm{e}^{\mathrm{i}\theta/2} & \sqrt{\frac{\xi-1}{2}}\mathrm{e}^{\mathrm{i}\theta/2} \\ \sqrt{\frac{\xi-1}{2}}\mathrm{e}^{-\mathrm{i}\theta/2} & \sqrt{\frac{\xi+1}{2}}\mathrm{e}^{-\mathrm{i}\theta/2} \end{pmatrix} \tag{10a}$$

and corresponding eigenvalues

$$\epsilon_k^b = \pm\sqrt{(\lambda_b + M_k)^2 - |\gamma_k|^2}, \tag{10b}$$

where $\xi_k = (\lambda_b + M_k)/\epsilon_k^b$ and θ is the phase of γ. The operators $\alpha_k^\dagger$ and $\beta_k^\dagger$ obey bosonic commutation relations.

If there exist wavevectors where the spectrum is gapless, however, a unitary transformation is required to diagonalize the Hamiltonian (6*b*). The eigenfunctions are then

$$\left(\zeta_k^\dagger, \eta_k^\dagger\right) = \left(b_{k\uparrow}^\dagger, b_{-k\downarrow}\right)\begin{pmatrix} (\mathrm{e}^{\mathrm{i}\theta/2})/\sqrt{2} & (\mathrm{e}^{\mathrm{i}\theta/2})/\sqrt{2} \\ (\mathrm{e}^{-\mathrm{i}\theta/2})/\sqrt{2} & (\mathrm{e}^{-\mathrm{i}\theta/2})/\sqrt{2} \end{pmatrix} \tag{11}$$

with eigenvalues of $2\lambda_b$ and 0. These operators obey the commutation relations, $[\zeta_k, \zeta_k^\dagger] = [\eta_k, \eta_k^\dagger] = 0$ and $[\zeta_k, \eta_k^\dagger] = [\eta_k, \zeta_k^\dagger] = 1$. The occupation of the Bose condensate is given by $n_0 = \sum_k \langle \eta_k^\dagger \eta_k \rangle$. As usual, the occurence of Bose–Einstein condensation means that the bosonic chemical potential is specified. In particular,

$$\lambda_b = 2\sum_{\alpha=x,y}\sqrt{J_\delta^2 D_\alpha^2/2 + (F_\alpha t + Q_\alpha J_\delta/4)^2} \tag{12a}$$

with the condensed modes being at

$$K_\alpha^0 = \tan^{-1}\left(\frac{-J_\delta D_\alpha/\sqrt{2}}{F_\alpha t + Q_\alpha J_\delta/4}\right). \tag{12b}$$

The physical interpretation of a gapless spectrum and Bose–Einstein condensation is that it signifies long-range magnetic order. The condensed bosons correspond to the classical spin component, while the normal bosons represent the zero-point quantum mechanical fluctuations. The pitch of the classical spiral is $2(K_x^0, K_y^0)$, which is readily related to the classical angle, θ (equation (5)). Absence of a Bose–Einstein condensate implies that the quantum mechanical fluctuations are dominant, leading to a disordered spin liquid with no long-range correlations.

Having determined the eigensolutions of (3) the self-consistent equations for the order parameters are obtained. These are, at zero temperature:

$$2-\delta = \frac{1}{N}\sum_{k}\left[\left(\frac{\lambda_b + M_k}{\epsilon_k^b}\right)(1-\delta_{kK_0}) + n_0\delta_{kK_0}\right] \tag{13a}$$

$$D_\alpha = \frac{J_\delta}{N}\sum_{k}\sin k_\alpha\left[\frac{(1-\delta_{kK_0})}{\epsilon_k^b} + \frac{n_0\delta_{kK_0}}{|\lambda_b + M_k|}\right]\sum_{\beta=x,y} D_\beta \sin k_\beta \tag{13b}$$

$$Q_\alpha = \frac{1}{N}\sum_{k}\cos k_\alpha\left[\left(\frac{\lambda_b + M_k}{\epsilon_k^b}\right)(1-\delta_{kK_0}) + n_0\delta_{kK_0}\right] \tag{13c}$$

$$F_\alpha = \frac{1}{N}\sum_{k\leqslant k_f}\cos k_\alpha \tag{13d}$$

and

$$\delta = \frac{1}{N}\sum_{k\leqslant k_f}. \tag{13e}$$

If Bose–Einstein condensation does exist (13*a*) can be regarded as defining n_0 with λ_b defined by (12). Otherwise, it defines λ_b. (13*e*) is a sum up to the Fermi wavevector for the fermions, and hence defines λ_f. The equations (13) are solved numerically, with the ground-state mean-field energy per site being given by [8],

$$E^{\mathrm{MF}} = -t(Q_xF_x + Q_yF_y) - J_\delta(D_x^2 + D_y^2) + J_\delta(Q_x^2 + Q_y^2)/4. \tag{14}$$

The resulting phase diagram is discussed in the next section.

3. The phase diagram

Figure 1 shows the diagram associated with the mean-field phases which minimize the energy. For zero doping the 2D Heisenberg antiferromagnet is stable. As holes are doped into the antiferromagnet the $(1,1)$ spiral develops. However, we note that the $(1,0)$ spiral is also very close in energy, *if isotropic D is not assumed*. For large t/J there is a rapid decrease in the classical nearest neighbour angle, $\theta_{ij} = \cos^{-1}(\hat{\Omega}_i \cdot \hat{\Omega}_j)$, while for small t/J the spins remain nearly antiferromagnetically aligned for quite large doping. Figure 2 illustrates the nearest neighbour classical angle as a function of doping for $t/J = 2.0$. For small deviations from Néel order the classical angle is given approximately by

$$\pi - \theta_{ij} \simeq \frac{\pi}{2}\frac{t}{J}\delta.$$

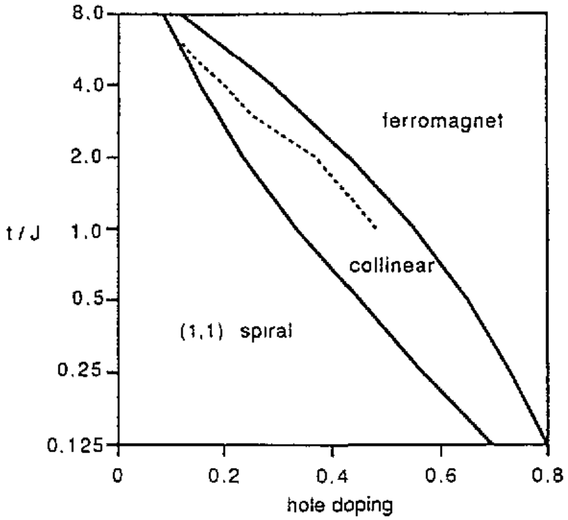

Figure 1. Mean-field phase diagram of the 't–J' model. The broken curve indicates the phase boundary line between the (1, 1) spiral and the flux phase as taken from [6].

Neutron scattering experiments would therefore give Bragg peaks at Q vectors $\pi(1 \pm t\delta/\sqrt{2}J, 1 \pm t\delta/\sqrt{2}J)$, which, although being in the wrong direction, have magnitudes in close agreement with experimental Q vectors of $\pi(1 \pm 2\delta, 1)$ and $\pi(1, 1 \pm 2\delta)$ for $La_{2-x}Sr_xCuO_4$ [1].

By allowing the order parameters to be anisotropic we find new energetically favourable phases. In particular, if one of the components of D is chosen to be zero, then the component of Q in the orthogonal direction is zero. This is the collinear phase in which the spins are aligned antiferromagnetically in one direction and ferromagnetically in the other. As the doping in increased there is a first-order transition to this collinear phase from the (1, 1) spiral. The collinear phase is stable for quite high doping before a further first-order phase transition to the ferromagnet phase occurs.

Chakraborty *et al* [6] introduced the so-called 'flux phase' which breaks time reversal invariance: $D_x = \mathrm{i}D_y$. They showed that this phase is more stable than the Nagaoka ferromagnet. Unfortunately, we were unable to find reliable mean-field solutions of this phase to test it against the collinear phase. However, the dashed line in figure 1 indicates the phase boundary line between the (1, 1) spiral and the flux phase as taken from [6]†. The position of this line indicates that the collinear phase is stable with respect to the (1, 1) spiral in parameter ranges where the flux phase is not stable.

Bose–Einstein condensation occurs in most regions of the phase diagram ,which implies long-range order. Figure 2 shows the fraction of condensed (i.e. classical) spins as a function of doping, defined by $2n_0/N + \delta$. As the doping is increased, and the spins become more ferromagnetically aligned, the classical component of the spins increases so that at the ferromagnetic regime there are no zero-point fluctuations. Notice that there are discontinuities in the condensed fraction at the phase boundaries. Bose–Einstein condensation is, however, an artefact of the mean-field calculation. If fluctuations in the

† These data were taken from [6] assuming that the J used in their calculation is the mean-field value of J i.e. $J(1-\delta)^2$

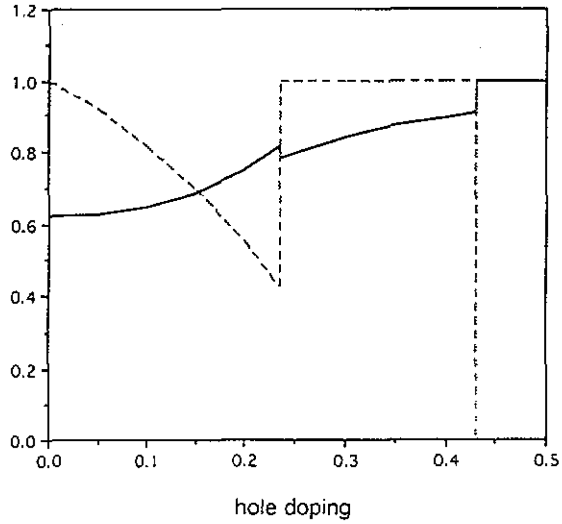

Figure 2. The nearest-neighbour classical angle, θ_{ij}/π (broken line), and the fraction of condensed (classical) spins (full curve) versus doping for $t/J = 2.0$. Note that in the collinear region θ_{ij} is π in one direction and 0 in the orthogonal direction.

phase of $\langle\Delta_{ij}\rangle$ are taken into account, which arise from the holes hopping across bonds, then long-range phase coherence would presumably be lost.

4. Conclusions

We have extended the Schwinger boson mean-field theories of the '*t–J*' model by allowing for anisotropic order parameters. This has two effects. First, the $(1, 1)$ and $(1, 0)$ spiral phases are now very close in energy. The inclusion of arbitrarily weak intrasublattice coupling may therefore stabilize the $(1, 0)$ spiral with respect to the $(1, 1)$ spiral, in agreement with the experimental observations. Second, a collinear phase, in which the spins are antiferromagnetically aligned in one direction and ferromagnetically aligned in the other, is found to be stable over a significant range of the phase diagram.

Acknowledgments

We thank the SERC (United Kingdom) for financial support (grant reference GR/F 75445). WB is grateful for a grant from the University of Sheffield Research Fund.

References

[1] Cheong S-W, Aeppli G, Mason T E, Mook H, Hayden S M, Canfield P C, Fisk Z, Clausen K N and Martinez J L 1991 *Phys. Rev. Lett.* **67** 1791
[2] Shraiman B I and Siggia E D 1989 *Phys. Rev. Lett.* **62** 1564
[3] Barford W and Lu J P 1991 *Phys. Rev.* B **43** 3540
[4] Lu J P, Si Q M, Kim J H and Levin K 1990 *Phys. Rev. Lett.* **65** 2466
[5] Yoshioka D 1989 *J. Phys. Soc. Japan* **58** 1516
Jayaprakash C, Krishnamurthy H R and Sarker S 1989 *Phys. Rev.* B **40** 2610

Kane C L, Lee P A, Ng T K, Chakraborty B and Read N 1990 *Phys. Rev.* B **41** 2653
[6] Chakraborty B, Read N, Kane C and Lee P A 1990 *Phys. Rev.* B **42** 4819
[7] Gan J and Mila F 1991 *Phys. Rev.* B **44** 12624
[8] For details of the Hubbard–Stratonovich transformations see
Auerbach A and Larson B E 1991 *Phys. Rev.* B **43** 7800
[9] Ring P and Schuck P 1980 *The Nuclear Many-Body Problem* (New York: Springer)